Protein Science (1995), *4*:1279–1290. Cambridge University Press. Printed in the USA.
Copyright © 1995 The Protein Society

Solution secondary structure of calcium-saturated troponin C monomer determined by multidimensional heteronuclear NMR spectroscopy

CAROLYN M. SLUPSKY,[1] FERNANDO C. REINACH,[2] LAWRENCE B. SMILLIE,[1] AND BRIAN D. SYKES[1]

[1] MRC Group in Protein Structure and Function, Department of Biochemistry, University of Alberta, Edmonton, Alberta T6G 2H7, Canada
[2] Department Bioquímica, Instituto de Química, Universidade de São Paulo, C.P. 20780 CEP 01498, São Paulo, Brazil

(RECEIVED February 14, 1995; ACCEPTED April 20, 1995)

Abstract

The solution secondary structure of calcium-saturated skeletal troponin C (TnC) in the presence of 15% (v/v) trifluoroethanol (TFE), which has been shown to exist predominantly as a monomer (Slupsky CM, Kay CM, Reinach FC, Smillie LB, Sykes BD, 1995, *Biochemistry 34*, forthcoming), has been investigated using multidimensional heteronuclear nuclear magnetic resonance spectroscopy. The ^{1}H, ^{15}N, and ^{13}C NMR chemical shift values for TnC in the presence of TFE are very similar to values obtained for calcium-saturated NTnC (residues 1–90 of skeletal TnC), calmodulin, and synthetic peptide homodimers. Moreover, the secondary structure elements of TnC are virtually identical to those obtained for calcium-saturated NTnC, calmodulin, and the synthetic peptide homodimers, suggesting that 15% (v/v) TFE minimally perturbs the secondary and tertiary structure of this stably folded protein. Comparison of the solution structure of calcium-saturated TnC with the X-ray crystal structure of half-saturated TnC reveals differences in the ϕ/ψ angles of residue Glu 41 and in the linker between the two domains. Glu 41 has irregular ϕ/ψ angles in the crystal structure, producing a kink in the B helix, whereas in calcium-saturated TnC, Glu 41 has helical ϕ/ψ angles, resulting in a straight B helix. The linker between the N and C domains of calcium-saturated TnC is flexible in the solution structure.

Keywords: NMR; structure; TFE; troponin C

Troponin C is the calcium-binding protein of the thin filament of muscle involved in the regulation of muscle contraction. Muscle contraction begins with the release of calcium from the sarcoplasmic reticulum. As the calcium concentration increases in the muscle cell, TnC binds calcium and undergoes a conformational change that is transmitted to other proteins in the thin filament, leading ultimately to muscle contraction. This calcium-mediated regulation is of wide interest and many biochemical and biophysical studies have been undertaken to characterize the conformational change between calcium-free and calcium-bound TnC (for a review, see Grabarek et al., 1992). Chicken skeletal TnC has 162 amino acid residues (for a molecular weight of 18,257) and binds four metal ions in four separate metal ion-binding sites numbered consecutively from the N-terminus of the protein. The structure of half-saturated avian skeletal TnC (with calcium binding sites III and IV filled) has been solved using X-ray crystallographic techniques (Herzberg & James, 1988; Satyshur et al., 1988, 1994) and reveals two domains (the C-terminal and the N-terminal domains), each with two EF-hand helix-loop-helix calcium binding sites. The C-terminal domain contains the high affinity calcium/magnesium binding sites, which have a K_{Ca} in the range of $2 \times 10^7\ M^{-1}$; these are referred to as the structural sites because they are always filled with calcium or magnesium in the muscle cell (Potter & Gergely, 1975). The N-terminal domain contains the lower affinity calcium-specific binding sites, which have a K_{Ca} in the range of $3 \times 10^5\ M^{-1}$; these are referred to as the regulatory sites because the

Reprint requests to: Brian D. Sykes, Department of Biochemistry, 474-Medical Sciences Building, University of Alberta, Edmonton, Alberta T6G 2H7, Canada; e-mail: bds@polaris.biochem.ualberta.ca.

Abbreviations: TnC, troponin C (unless otherwise stated, calcium-saturated recombinant chicken skeletal troponin C, which has three residues different from turkey skeletal TnC: A1 versus P1, I130 versus T130, and D133 versus E133); NTnC, N-terminal domain of troponin C (residues 1–90); SCIII, synthetic peptide calcium binding site III of TnC (93–126); TH2, proteolytically derived calcium binding site IV of TnC (121–159 of rabbit skeletal TnC); TFE, trifluoroethanol; CSI, chemical shift index; NOESY, nuclear Overhauser enhancement spectroscopy; TOCSY total correlation spectroscopy; HSQC, heteronuclear single quantum coherence; HMQC, heteronuclear multiple-quantum coherence.

binding of calcium to these sites in skeletal muscle regulates muscle contraction (Potter & Gergely, 1975; Li et al., 1995). Knowledge of the structure of TnC in its half and fully calcium-saturated forms is essential to understanding the molecular mechanism of muscle contraction.

A model for the calcium-induced conformational change for the N-domain of TnC has been proposed (Herzberg et al., 1986) based on the structure of the C-domain of TnC. This model suggests that, when calcium binds to sites I and II, the major conformational transition is a movement of the B/C helix pair away from the A/D helix pair, exposing a patch of hydrophobic residues, providing a binding site for other muscle proteins. This model has strong support from several lines of evidence, including NMR (Levine et al., 1977, 1978; Evans et al., 1980; Gagné et al., 1994) and site-directed mutagenesis (Fujimori et al., 1990; Grabarek et al., 1990; Gusev et al., 1991; Pearlstone et al., 1992a, 1992b). There have been several studies of TnC that have focused on the function of the central helix (Reinach & Karlsson, 1988; Xu & Hitchcock-DeGregori, 1988; Gulati et al., 1990, 1993; Dobrowolski et al., 1991; Babu et al., 1993; Wang et al., 1993). These studies have served to illustrate that the central helix of TnC is essential for TnC function, and that the helix is not as rigid as suggested by the crystal structure, although the long helix is extended in the model of the complex between TnC and TnI recently proposed from small-angle X-ray scattering (Olah & Trewhella, 1994). Calmodulin is a protein with structural characteristics very similar to TnC (Means & Dedman, 1980). Calmodulin has been shown to have a flexible linker between the two domains, allowing the molecule to become more compact upon binding calcium (Barbato et al., 1992). TnC has also been reported to become more compact upon binding calcium, most likely due to flexibility in the long central helix (Heidorn & Trewhella, 1988; Gulati et al., 1993; Wang et al., 1993). In order to elucidate the details of the structural change from the apo to the calcium-saturated form of TnC, and to study the apparent flexibility of the central helix, we have initiated an NMR study of this protein.

NMR spectroscopy has developed into a technique capable of determining 3D structures of proteins in solution. The sequential resonance assignment of the backbone protons is the prerequisite for determining the 3D structure. Sequential assignment has most commonly been accomplished by means of homonuclear interresidue through-space correlations coupled with homonuclear intraresidue through-bond correlations (Wüthrich, 1986). NMR of proteins has previously been limited to molecular weights less than 15,000 Da due to the complexity of 2D homonuclear spectra and the fact that linewidths increase rapidly as the size of the molecule increases. Developments in molecular biology have allowed not only large amounts of proteins to be expressed but have allowed the incorporation of ^{15}N and ^{13}C isotope labels into proteins. The field of NMR has since exploded with a variety of 3D and 4D techniques that are extensions of 2D techniques, allowing spectral editing and internuclear correlations based on the attached heteronuclei, and thus can achieve better resolution than 2D methods. These methods may also be grouped into either NOESY-type (e.g., the ^{13}C-edited NOESY [Ikura et al., 1990b] or ^{15}N-edited NOESY [Marion et al., 1989b]) or COSY-type (e.g., the ^{15}N-edited TOCSY [Marion et al., 1989a], the CT-HNCA, CT-HNCO, and CT-HN(CO)CA experiments [Grzesiek & Bax, 1992], the HCACO experiment [Powers et al., 1991], or the HCCH-COSY experiment [Bax et al., 1990a, 1990b]). These new methods also represent new strategies for assignment of proteins based on the attached heteronucleus (Garrett et al., 1991; Meadows et al., 1994) and complement very well the "traditional" sequential assignment procedure. It is now feasible to solve the structure of proteins up to the size of 25,000 Da (Clore & Gronenborn, 1991; Wagner, 1993; Gronenborn & Clore, 1994). Our goal has been to use these new techniques to solve the 3D solution structure of fully calcium-saturated TnC.

TnC, at physiological pH, has previously been shown by ultracentrifugation techniques (Murray & Kay, 1972; Margossian & Stafford, 1982) to undergo a reversible calcium-induced aggregation. At the concentration required for NMR observation, the calcium-saturated state of TnC in water shows NMR resonance linewidths of the N-domain indicative of aggregation (Slupsky et al., 1995). Better linewidths can be achieved at high temperatures (Slupsky et al., 1995); however, many resonances were lost due to amide exchange with the solvent. Varying pH and salt concentrations had minimal effect on reducing the aggregation problem (C.M. Slupsky, unpubl. results). The titration of calcium-saturated TnC with TFE revealed a set of resonances that were largely unaffected by the addition of TFE. These resonances corresponded to the C-terminal domain resonances. Another set of resonances, corresponding to the N-terminal domain resonances, experienced a decrease in ^{1}H linewidth and an increase in intensity upon addition of TFE (Slupsky et al., 1995). The interface for the dimer was shown to involve two N-terminal domains from two separate TnC monomers. Further, it was shown that residues located at the end of helix B and the end of helix C, which had significant changes in their chemical shifts, were the residues involved in dimer interface (Slupsky et al., 1995). In the presence of 15% (v/v) TFE at 40 °C, ultracentrifugation and NMR data illustrated that TnC behaves essentially like a monomeric unit (Slupsky et al., 1995).

The present NMR study deals with an overexpressed and isotopically labeled form of cloned chicken skeletal TnC in its monomeric form in the presence of 15% (v/v) TFE. Cysteine 101 of TnC was reacted with iodoacetamide to prevent oxidation and thus avoid aggregation. A detailed account of the secondary structure of TnC derived from NOE data, coupling constant information, and CSI data based upon the assignment of the backbone residues is presented. It will be shown that the secondary structure of TnC is minimally perturbed with use of TFE as a denaturant of quaternary structure, and that the TnC monomer secondary structure is essentially equivalent to the TnC dimer secondary structure. Finally, comparisons will be made to the X-ray crystal structure of half-saturated TnC.

Results

Resonance assignment strategy

Assignment of the ^{1}H, ^{13}C, and ^{15}N NMR resonances of the backbone nuclei of TnC made use of the four 3D triple-resonance NMR experiments HNCA, HN(CO)CA, HNCO, and HCACO, in conjunction with ^{15}N-edited NOESY and ^{15}N-edited TOCSY experiments. Figure 1 presents a portion of the ^{1}H–^{15}N-HSQC NMR spectrum of TnC in the presence of 15% TFE, illustrating the most crowded region of the spectrum and the severe overlap in the ^{15}N and ^{1}H dimensions for this protein. There are 113 of the 158 observable amide to proton correlations in this

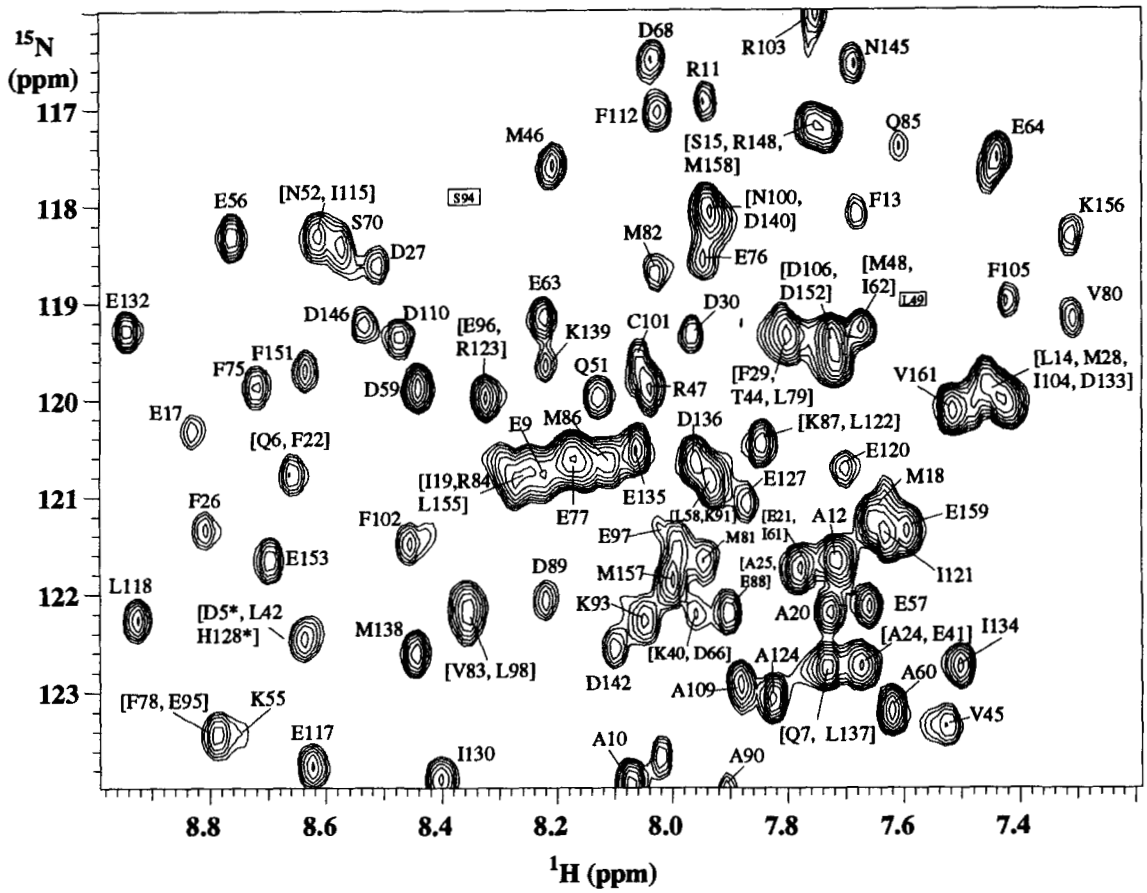

Fig. 1. 2D ^{1}H-^{15}N-HSQC NMR spectrum of ^{15}N-labeled TnC showing the most crowded region of the spectrum. Residues shown in square brackets are degenerate. Residues marked with an asterisk are tentative assignments. Boxes are placed in the spectrum where correlations were found using 3D techniques but were not present in this spectrum.

region of the spectrum. Unobservable amide to proton correlations included A1, S2, and M3, which have fast amide proton exchange rates, and one proline (P53), which does not have an amide hydrogen. Of these 113 correlations, 43 are overlapping. The residues that are overlapping are shown in square brackets in Figure 1. Fourteen correlations are composites of overlapping pairs of ^{15}N-^{1}HN crosspeaks, four correlations are threefold degenerate, and one correlation is fourfold degenerate. Most of the ^{1}H-^{15}N degeneracies could be resolved in at least one of either the HNCA, HN(CO)CA, or HNCO spectra. The ^{1}H-^{15}N assignments for D5 and H128 are tentative and based on a previous assignment of TnC in the absence of TFE, and these are shown by asterisks. These residues were not seen in any of the HNCA, HNCO, or HN(CO)CA experiments possibly due to fast amide exchange. The resonances of L49 and S94 were unobservable in this 2D ^{15}N-^{1}H HSQC spectrum, and their positions are indicated in the figure. L49 and S94 were observed in the 3D HNCA, and the 3D HN(CO)CA spectra, whereas only L49 was observed in the 3D HNCO spectrum. Both were observed in the ^{15}N-edited NOESY spectrum and the ^{15}N-edited TOCSY spectrum.

Sequential assignment was achieved in several steps. Initially, possible amino acid spin systems were identified as arising from either the N-domain or the C-domain based on a calcium titration using 1D and 2D homonuclear NMR as a monitor (data not shown) and on previous partial assignments of TnC (Tsuda et al., 1988, 1990). These possible assignments were obtained by observing the differing exchange phenomena in the N- and C-terminal domains upon binding calcium ions. The C-terminal domain of TnC contains the high affinity calcium binding sites and the N-terminal domain of TnC contains the low affinity calcium binding sites (Potter & Gergely, 1975). During a calcium titration, where the calcium is increased from 0 to 2 mol of calcium per mole of protein, a signal corresponding to the unbound state gradually decreases in intensity with a concomitant increase in intensity of a signal at a different chemical shift value corresponding to the calcium-bound state. Thus, the C-domain exhibits slow chemical exchange. When the calcium concentration is increased from 2 to 4 mol of calcium per mole of protein, the signals gradually move across the spectrum, at each point the chemical shift value being an average of the bound and unbound states. Thus, the N-domain exhibits fast chemical exchange. After identifying a few of these "starting places," the ^{1}HN and ^{15}N assignments were identified on an ^{15}N-^{1}H-HSQC NMR spectrum. Sequential connectivities along the backbone were then made using an approach similar to the one devised for sequential assignment of the homologous protein calmodulin (Ikura et al., 1990a), starting with the residues for which the ^{15}N and ^{1}H assignments were known. This approach involves combining the intraresidue ^{1}HN(i)-^{15}N(i)-^{13}Cα(i), ^{1}Hα(i)-

$^{13}C\alpha(i)$-$^{13}C'(i)$, and $^{1}HN(i)$-$^{15}N(i)$-CαH correlations with the sequential interresidue $^{1}HN(i)$-$^{15}N(i)$-$^{13}C\alpha(i-1)$, $^{1}HN(i)$-$^{15}N(i)$-$^{13}C'(i-1)$, and $d_{NN}(i \pm 1)$ correlations. Due to resonance overlap, many of the connectivities were not unique.

Figure 2 represents expansions of 2D contour plots at selected ^{15}N frequencies of the 3D HNCA, HN(CO)CA, HNCO, ^{15}N-edited NOESY, and ^{15}N-edited TOCSY experiments, as well as selected $^{13}C'$ frequencies of the HCACO experiment, illustrating the sequential assignment procedure using all six of these experiments. Details of the assignment can be found in the Materials and methods. In Figure 2, the sequential assignment for residues D150 to N145 are shown. For β-sheet regions, the d_{NN} NOE is either very weak or unobservable (Wüthrich, 1986). Starting at residue D150 (which is in an antiparallel β-sheet structure in calcium binding site IV), the HNCA spectrum shows an intense crosspeak for the intraresidue correlation and a weak crosspeak for the interresidue correlation. At the same ^{15}N (130.0 ppm) and ^{1}HN (9.29 ppm) frequencies, the $^{13}C\alpha(i-1)$ correlation (to I149) may be found in the HN(CO)CA spectrum, and the $^{13}C'(i-1)$ assignment (to I149) may be found in the HNCO spectrum. The $^{13}C\alpha(i-1)$ and $^{13}C'(i-1)$ frequency information obtained from D150 for I149 may be used to search the HCACO experiment to find the $^{1}H\alpha$ frequency of I149. Because there are no NOESY $d_{NN}(i \pm 1)$ correlations, ^{15}N planes must be searched in the ^{15}N-edited TOCSY and HNCA experiments, and all ^{1}HN frequencies that correlate the $^{1}H\alpha$ and $^{13}C\alpha$ chemical shifts of I149 must be found. Fortunately, this procedure yielded only one possibility, and therefore the sequential assignment procedure could be continued from I149 in the same way to obtain the ^{15}N, ^{1}HN, $^{13}C\alpha$, $^{13}C'$, and $^{1}H\alpha$ chemical shift values for R148. A $d_{NN}(i-1)$ is observable in the ^{15}N-edited NOESY spectrum of R148, making the assignment from R148 to G147 easier because ^{15}N planes at a particular ^{1}HN frequency need only be sampled. Very weak crosspeaks are found for G147 Hα atoms (and all glycine Hα atoms) in the HCACO experiment due to the fact that they are only weakly excited because they are so far upfield in the Cα region. The TOCSY transfer of magnetization to G147 α-protons was also very poor possibly due to the fact that G147 is very far downfield (10.38 ppm) in the ^{1}HN dimension. Assignment of G147 (even without the presence of the $^{1}H\alpha$ chemical shifts in the ^{15}N-edited TOCSY) could be continued because a $d_{NN}(i, i-1)$ from R148 to G147 was found and only one $d_{NN}(i, i+1)$ could be found in all the ^{15}N planes of the ^{15}N-edited NOESY to link G147 to R148. At this ^{15}N and ^{1}HN frequency, the $^{13}C\alpha$ shift for G147 found on the HNCA corresponded to the $^{13}C\alpha$ shift suggested for G147 by R148. The assignment from G147 to D146 and D146 to N145 using $d_{NN}(i-1)$, $^{13}C\alpha(i-1)$, $^{13}C'(i-1)$, and $^{1}H\alpha(i-1)$ information obtained from the experiments was straightforward. Using all six experiments, the complete assignment of the backbone chemical shifts for TnC were obtained and are shown in Table 1.

Secondary structure determination

Secondary structure elements in proteins have distinct NOE connectivity patterns as described by Wüthrich (1986). Helices may be characterized by the existence of $d_{\alpha N}(i, i+3)$, $d_{\beta N}(i, i+3)$, $d_{\alpha\beta}(i, i+3)$, and strong $d_{NN}(i, i+1)$ connectivities, whereas β-sheets are characterized by strong $d_{\alpha N}(i, i+1)$ and the absence of $d_{NN}(i, i \pm 1)$ connectivities. A new method for characterizing helices is the ratio of the $d_{N\alpha}/d_{\alpha N}$ (Gagné et al., 1994) (where $d_{\alpha N}$ refers to the NOE involving the Hα of residue $i-1$ to the HN of residue i, and $d_{N\alpha}$ refers to the NOE between HN of residue i and Hα of residue i). α-Helices are characterized by a $d_{N\alpha}/d_{\alpha N}$ ratio greater than one, whereas β-sheets are characterized by a $d_{N\alpha}/d_{\alpha N}$ ratio less than one. In a simulation where spin-diffusion is taken into account and compared to the results using a two-spin approximation (data not shown), it was observed that all $d_{N\alpha}/d_{\alpha N}$ ratios tended to unity as the amount of spin-diffusion increased, regardless of the type of secondary structure. It follows, therefore, that the measured $d_{N\alpha}/d_{\alpha N}$ ratio underestimates the amount of α-helix or β-sheet present. In addition to the ratio of the $d_{N\alpha}/d_{\alpha N}$, there is a strong correlation between the deviations of $^{13}C\alpha$, $^{13}C'$, and $^{1}H\alpha$ chemical shifts from their random-coil values with the secondary structure of the protein (Wishart et al., 1991a, 1991b). For α-helices, positive deviations from random coil values occur for the $^{13}C\alpha$ and $^{13}C'$ shifts and negative deviations occur for the Hα shifts. For β-sheets, negative deviations from random coil values occur for the $^{13}C\alpha$ and $^{13}C'$ shifts and positive deviations occur for the $^{1}H\alpha$ shifts. α-Helices may also be characterized by small HN-Hα J couplings due to the smaller dihedral angle between the HN and Hα protons, whereas β-sheets have large HN-Hα J couplings due to the larger dihedral angle between the HN and Hα protons. Because of significant overlap in the ^{15}N-edited NOESY spectrum, four of these data (the $d_{\alpha N}(i, i+3)$ NOEs, the $d_{N\alpha}/d_{\alpha N}$ ratio, the CSI, and the J-coupling data) taken together were used to define the secondary structure of TnC as illustrated in Figure 3. Also shown are the slowly exchanging amide hydrogens that indicate buried or hydrogen bonded amide hydrogens. Of the unambiguously assigned residues, the slowly exchanging amide resonances are F26, A20, D30, I37, L42, V45, M46, E63, I73, D74, E77, M82, F105, G111, F112, I113, D114, L118, I149, D150, E153, and F154. The slowest exchanging amide resonances are F26, F105, F112, L118, and F154. These data are similar to those obtained for calmodulin (Ikura et al., 1991), where it was found that the calcium binding loops of the C-terminal domain exchange slower than the calcium binding loops of the N-terminal domain, suggesting that the calcium binding loops of the C-terminal domain are more stable in their conformation than the calcium binding loops of the N-terminal domain.

The data in Figure 3 identify the location of nine helices, four calcium binding loops and four short β-strands. The helices span the regions (N) Asp 5–Phe 13, (A) Glu 16–Phe 29, (B) Thr 39–Met 48, (C) Lys 55–Glu 64, (D) Phe 75–Arg 84, (E) Asp 89–Phe 105, (F) Glu 116–Ala 124, (G) Glu 131–Ser 141, and (H) Phe 151–Gly 160. The beginnings and endings of the helices are marked by changes in one or more of the CSI, the $d_{N\alpha}/d_{\alpha N}$ ratio, and the J-coupling. The only ambiguity occurred in the central region between the two domains where it appears that the secondary structure is mainly helical; however, T_2 data (Slupsky et al., 1995) have shown that three residues (M86–E88) are flexible. Q85 appears to have a CSI and $^{3}J_{HNH\alpha}$ indicative of β-sheet type secondary structure. The helices were thus broken up at R84 and restarted at D89. The crystal structure of half-saturated TnC reveals similar starts and stops of helices (Herzberg & James, 1988; Satyshur et al., 1988, 1994) except for the ends of some helices and in the linker region between the two domains where the helix is contiguous in the crystal structure (from F75 to F105). One residue of particular interest, is the residue Glu 41. This residue was found to have "irregular" non-

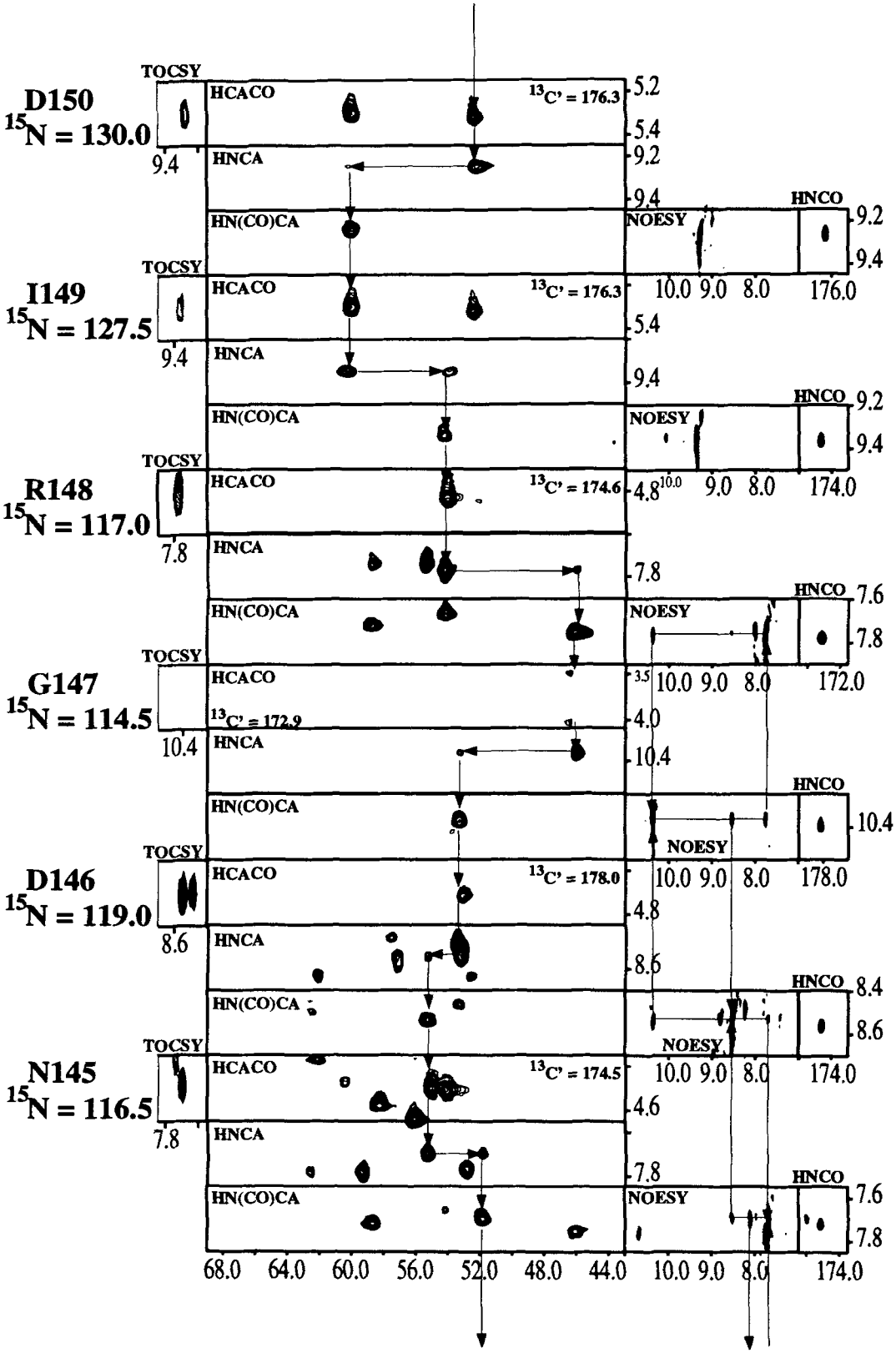

Fig. 2. ^{1}H-$^{13}C\alpha$ planes extracted from HCACO, HNCA, HN(CO)CA, and HNCO experiments, and ^{1}H-^{1}H planes extracted from ^{15}N-edited TOCSY, and ^{15}N-edited NOESY spectra at selected ^{15}N (HNCA, HN(CO)CA, HNCO, ^{15}N-edited TOCSY, and ^{15}N-edited NOESY) and $^{13}C'$ (HCACO) frequencies, showing the sequential assignment for a set of six residues (D150-N145). Shown are the $^{13}C\alpha$-^{1}HN correlations of the HNCA and HN(CO)CA, the $^{13}C\alpha$-$^{1}H\alpha$ correlations for the HCACO, the $^{13}C'$-^{1}HN correlations for the HNCO, the ^{1}HN-^{1}HN correlations for the ^{15}N-edited NOESY, and the ^{1}HN-$^{1}H\alpha$ correlations for the ^{15}N-edited TOCSY.

Table 1. *Backbone chemical shifts of resonances of skeletal troponin C*[a]

Residue	Chemical shift (ppm)					Residue	Chemical shift (ppm)				
	^{15}N	NH	^{13}Cα	CαH	^{13}CO		^{15}N	NH	^{13}Cα	CαH	^{13}CO
A1			52.1	4.12	174.6	I61	121.7	7.80	65.5	3.68	178.0
S2			58.3	4.57	174.5	I62	119.2	7.68	65.1	3.49	177.8
M3			55.3			E63	119.1	8.24	59.5	4.03	178.6
T4	114.8	8.03	62.4	4.35	175.0	E64	117.6	7.46	59.1	4.11	178.2
D5	122.6*	8.66*	57.6	4.34	179.0	V65	112.0	7.49	62.2	4.36	176.2
Q6	120.8	8.72	59.6	4.02	179.0	D66	122.3	7.98	54.1	4.62	176.9
Q7	122.8	7.80	58.2	4.04	177.7	E67	129.5	8.55	58.9	4.30	177.2
A8	124.2	8.19	55.2	4.20	180.5	D68	116.6	8.05	52.7	4.73	177.8
E9	120.8	8.16	58.6	4.14	178.4	G69	110.2	7.74	47.2	3.92, 3.81	175.4
A10	123.8	8.07	54.8	4.14	178.8	S70	118.5	8.59	60.2	4.23	176.2
R11	117.1	7.96	59.0	3.78	177.8	G71	117.6	10.79	45.7	4.12, 3.44	172.6
A12	121.1	7.72	53.7	4.20	179.1	T72	108.7	7.70	58.3	4.90	173.7
F13	118.2	7.70	58.7	4.54	175.4	I73	126.9	9.27	60.6	5.07	176.2
L14	120.0	7.44	54.0	4.40	176.0	D74	131.8	9.48	53.2	5.27	176.0
S15	117.3	7.70	56.6	4.65	175.2	F75	119.9	8.74	61.8	3.63	176.5
E16	123.2	9.09	60.6	3.96	179.0	E76	118.4	7.94	60.0	3.89	179.2
E17	120.4	8.85	60.1	4.05	179.0	E77	120.6	8.20	58.5	4.20	179.0
M18	120.9	7.66	58.6	4.07	178.4	F78	123.5	8.80	61.5	4.05	176.7
I19	120.8	8.27	67.3	3.76		L79	119.3	7.82	58.4	3.42	178.7
A20	122.2	7.76	55.2	4.10	181.1	V80	119.1	7.33	67.4	3.35	178.0
E21	121.8	7.77	59.6	4.20	179.9	M81	121.7	7.95	59.2	3.81	178.2
F22	120.8	8.68	59.5	4.94	178.8	M82	118.9	8.05	56.7	4.11	179.2
K23	124.6	9.22	58.6	4.02	177.4	V83	122.3	8.41	67.3	3.63	178.3
A24	122.8	7.70	54.4	4.15	179.6	R84	120.9	8.25	60.4	3.84	179.0
A25	122.2	7.94	55.2	4.07	178.3	Q85	117.5	7.60	54.4	4.58	175.8
F26	121.3	8.82	62.6	3.17	176.9	M86	120.4	8.00	58.0	4.21	177.5
D27	118.6	8.55	57.2	4.20	178.2	K87	120.4	7.88	57.8	4.11	177.1
M28	120.0	7.43	58.3	4.08	178.0	E88	122.3	7.94	58.6	4.14	178.4
F29	119.4	7.81	58.8	4.23	177.9	D89	122.1	8.24	56.1	4.57	177.5
D30	119.2	7.98	52.3	4.51	176.9	A90	124.0	7.93	53.8	4.25	179.0
A31	130.8	7.71	55.2	4.08	179.3	K91	120.9	7.92	58.1	4.21	178.0
D32	114.4	8.25	53.0	4.59	177.9	G92	110.0	8.23	46.0	4.01	175.2
G33	111.6	8.00	47.0	3.86	175.9	K93	122.2	8.08	57.3	4.41	177.6
G34	109.6	8.16	46.5	4.08, 3.98	176.1	S94	117.9	8.36	59.7	4.48	175.7
G35	113.8	10.69	45.3	4.47, 3.65	173.3	E95	123.7	8.80	60.4	4.08	178.4
D36	116.2	7.78	52.8	5.16	173.4	E96	120.1	8.32	59.6	4.11	179.1
I37	126.4	9.64	60.2	4.96	176.0	E97	121.6	8.04	59.6	4.18	179.9
S38	124.1	8.77	56.0	4.87	175.9	L98	122.2	8.37	58.4	4.34	179.5
T39	115.8	9.09	66.6	3.77	177.7	A99	124.5	8.61	55.5	4.12	179.9
K40	122.3	7.93	59.6	4.07	179.9	N100	118.2	7.96	56.5	4.46	177.4
E41	122.7	7.71	58.6	4.04	179.5	C101	119.5	8.12	59.0	4.09	175.5
L42	122.2	8.64	58.1	4.09	178.8	F102	121.4	8.47	62.5	3.32	176.3
G43	106.6	8.62	48.2	3.88, 3.64	175.4	R103	116.1	7.78	59.2	4.00	178.4
T44	119.5	7.80	67.5	3.90	176.3	I104	120.0	7.45	64.1	3.65	177.7
V45	123.0	7.53	67.0	3.50	177.8	F105	119.1	7.47	58.2	4.42	177.0
M46	117.6	8.23	59.6	4.00	178.9	D106	119.5	7.74	52.4	4.48	177.1
R47	120.0	8.07	59.1	4.69	181.4	K107	127.5	7.62	59.2	4.00	178.1
M48	119.2	7.72	59.0	4.22	177.7	N108	115.0	8.03	51.8	4.72	174.4
L49	119.0	7.58	55.1	4.37	177.7	109	122.9	7.89	53.2	4.08	176.6
G50	108.3	7.84	45.8	4.26, 3.77	174.8	D110	119.5	8.48	53.3	4.70	177.5
Q51	120.0	8.14	54.2	4.51	174.4	G111	113.7	10.42	45.2	3.99, 3.38	172.4
N52	118.0	8.60	51.2	5.16	172.2	F112	117.0	8.03	56.0	5.44	175.0
P53			62.8	4.76	177.6	I113	127.4	10.07	59.8	4.96	176.1
T54	113.5	8.48	60.4	4.52	175.5	D114	130.2	9.00	52.3	4.98	176.5
K55	123.2	8.76	60.4	3.88	178.1	I115	118.4	8.64	64.8	3.97	177.3
E56	118.4	8.77	60.8	4.09	180.0	E116	125.1	7.93	59.5	4.12	180.3
E57	122.2	7.70	59.5	4.00	179.3	E117	123.8	8.66	59.2	4.07	179.8
L58	120.9	7.94	58.1	4.04	178.8	L118	122.3	8.94	57.9	4.01	178.9
D59	119.9	8.46	57.5	4.34	179.0	G119	106.0	8.13	47.9	3.99, 3.65	175.5
A60	123.2	7.65	55.1	4.19	180.1	E120	120.9	7.64	59.7	4.10	179.3

(*continued*)

Table 1. *Continued*

Residue	Chemical shift (ppm)					Residue	Chemical shift (ppm)				
	^{15}N	NH	$^{13}C\alpha$	CαH	^{13}CO		^{15}N	NH	$^{13}C\alpha$	CαH	^{13}CO
I121	121.3	7.61	64.6	3.49	178.8	D142	122.7	8.09	53.1	4.62	176.8
L122	120.4	7.87	57.9	4.02	180.2	K143	126.6	8.02	57.0	4.24	177.8
R123	120.0	8.34	59.4	4.15	179.1	N144	115.4	8.13	51.7	4.85	175.0
A124	123.1	7.84	54.3	4.28	179.2	N145	116.8	7.71	55.1	4.49	174.5
T125	108.6	7.63	63.0	4.32	175.9	D146	119.2	8.55	53.1	4.71	178.0
G126	110.4	7.80	45.6	4.15, 3.88	174.2	G147	114.3	10.38	46.0	4.02, 3.47	172.9
E127	121.1	7.91	56.1	4.31	176.2	R148	117.1	7.77	54.1	4.83	174.6
H128	122.5*	8.66*	56.2	4.64	174.5	I149	127.4	9.37	60.0	5.30	176.3
V129	124.4	7.83	61.8	4.26	175.4	D150	129.8	9.29	52.5	5.32	176.3
I130	123.9	8.41	60.4	4.50	177.3	F151	119.9	8.66	62.0	3.72	176.5
E131	126.1	8.93	61.1	3.85	178.6	D152	119.4	7.75	58.1	4.19	179.9
E132	119.4	8.96	60.0	4.07	178.0	E153	121.8	8.71	59.0	4.00	180.1
D133	119.9	7.47	56.9	4.53	178.8	F154	126.1	9.17	61.5	4.27	176.7
I134	122.8	7.53	65.0	3.58	177.6	L155	120.8	8.28	58.4	3.57	180.1
E135	120.5	8.07	60.2	3.85	179.0	K156	118.2	7.31	58.5	4.03	177.4
D136	120.5	7.97	57.7	4.40	178.2	M157	121.8	8.03	58.7	4.08	179.2
L137	122.7	7.75	58.0	4.22	180.5	M158	117.2	7.78	55.3	4.35	178.2
M138	122.7	8.46	58.4	4.26	177.6	E159	121.4	7.52	58.4	4.08	177.9
K139	119.4	8.24	59.6	4.10	179.3	G160	108.4	7.98	45.7	4.06, 3.91	174.4
D140	118.2	7.96	56.8	4.48	177.6	V161	120.2	7.56	62.8	4.14	175.4
S141	114.2	7.75	60.4	4.49	174.3	Q162	129.3	7.73	57.7	4.18	180.7

[a] ^{1}H chemical shifts are referenced to internal DSS at 0.0 ppm, ^{13}C chemical shifts are referenced to external DSS at 0.0 ppm, and ^{15}N chemical shifts are referenced to external $^{15}NH_4Cl$ at 24.93 ppm. Chemical shifts are for *E. coli*-expressed chicken skeletal TnC (1.4 mM) (modified at cysteine 101 with a carboxamidomethyl group) in 150 mM KCl, 16 mM $CaCl_2$, 15% (v/v) TFE at pH 7.0 and 40 °C. Residues marked with * are tentative assignments.

helical ϕ/ψ angles ($\phi = -96°$; $\psi = -7°$) in the crystal structure and was shown to form a "kink" in helix B of the crystal structure where the N-domains are free of calcium (Herzberg & James, 1988; Satyshur et al., 1988, 1994). The calcium-saturated TnC structure presented here has no indication of ϕ/ψ angles for residue Glu 41 other than helix, suggesting that this residue has shifted its ϕ/ψ angles to better fit into a helix in the calcium-saturated form. This result was also verified for the calcium-saturated isolated N-domain, NTnC (Gagné et al., 1994).

The four β-sheet regions span residues 36–38, 72–74, 112–114, and 148–150. The β-sheets are in an antiparallel conformation (36–38 is antiparallel to 72–74, and 112–114 is antiparallel to 148–150) as observed by the presence of $d_{\alpha\alpha}$, d_{NN}, and $d_{\beta N}$ NOEs across the β-sheet ($d_{\alpha\alpha}$ for D36–D74, S38–T72 [these $^{1}H\alpha$ resonances overlap], F112–D150, and D114–R148; d_{NN} for I37–I73 and I113–I149; and $d_{\beta N}$ for I37–I73 and I113–I149), as was also observed for the symmetric homodimers in solution (Shaw et al., 1990; Kay et al., 1991). The calcium binding loops are well characterized by X-ray crystallographic studies (Herzberg & James, 1988; Satyshur et al., 1988, 1994) and consist of 12 residues flanked by α-helices in the typical EF-hand configuration. The calcium binding loops are comprised of the residues (I) Asp 30–Glu 41, (II) Asp 66–Glu 77, (III) Asp 106–Glu 117, and (IV) Asp 142–Glu 153. The first four residues in the C-terminal calcium binding loops (D106–A109 and D142–N145) are in a type I turn conformation as evidenced by strong NOEs between K107 NH (or K143 NH) and N108 NH (or N144 NH), N108 NH (or N144 NH) and A109 NH (or N145 NH), and K107 Hα (or K143 Hα) and A109 NH (or N145 NH). The equivalent residues in the N-terminal domain (D30–G33 and D66–G69), however, do not exhibit the $d_{\alpha N}(i, i+2)$ NOEs of the H$\alpha(i+1)$ to the NH$(i+3)$ residues in the loop.

There are four connecting loops in calcium-saturated TnC. These comprise residues Leu 14–Ser 15 (between the N helix and helix A), residues Gln 51–Thr 54 (between helix B and helix C), Gln 85–Glu 88 (between helix D and helix E), and residues Thr 125–Ile 130 (between helix F and helix G). T_2 data (Slupsky et al., 1995) suggest that the only flexible linker region is that between helices D and E, as well as F and G. The linker in the N-domain (between helices B and C) does not appear flexible on the time scale of the T_2 experiment. Similar results were obtained for calmodulin, which has similar linker regions (Barbato et al., 1992).

Discussion

The data presented provide the first structural data for fully calcium-saturated TnC. In determining the secondary structure of TnC, a combination of the $d_{\alpha N}(i, i+3)$, the CSI, the J-coupling data, and the $d_{N\alpha}/d_{\alpha N}$ ratio were used. The distance corresponding to the $d_{N\alpha}$ is virtually the same for both the α-helix and the β-sheet (between 2.7 and 3.05 Å), where 96% of the distances corresponding to the $d_{N\alpha}$ NOE are in this range and 96% of the distances corresponding to the $d_{\alpha N}$ NOE are out of this range (S.M. Gagné, pers. comm.). The distance corresponding to the $d_{\alpha N}$ NOE varies depending on the type of secondary structure. The $d_{\alpha N}$ NOE in β-sheets is more intense than in α-helices because the α-proton of one residue is very

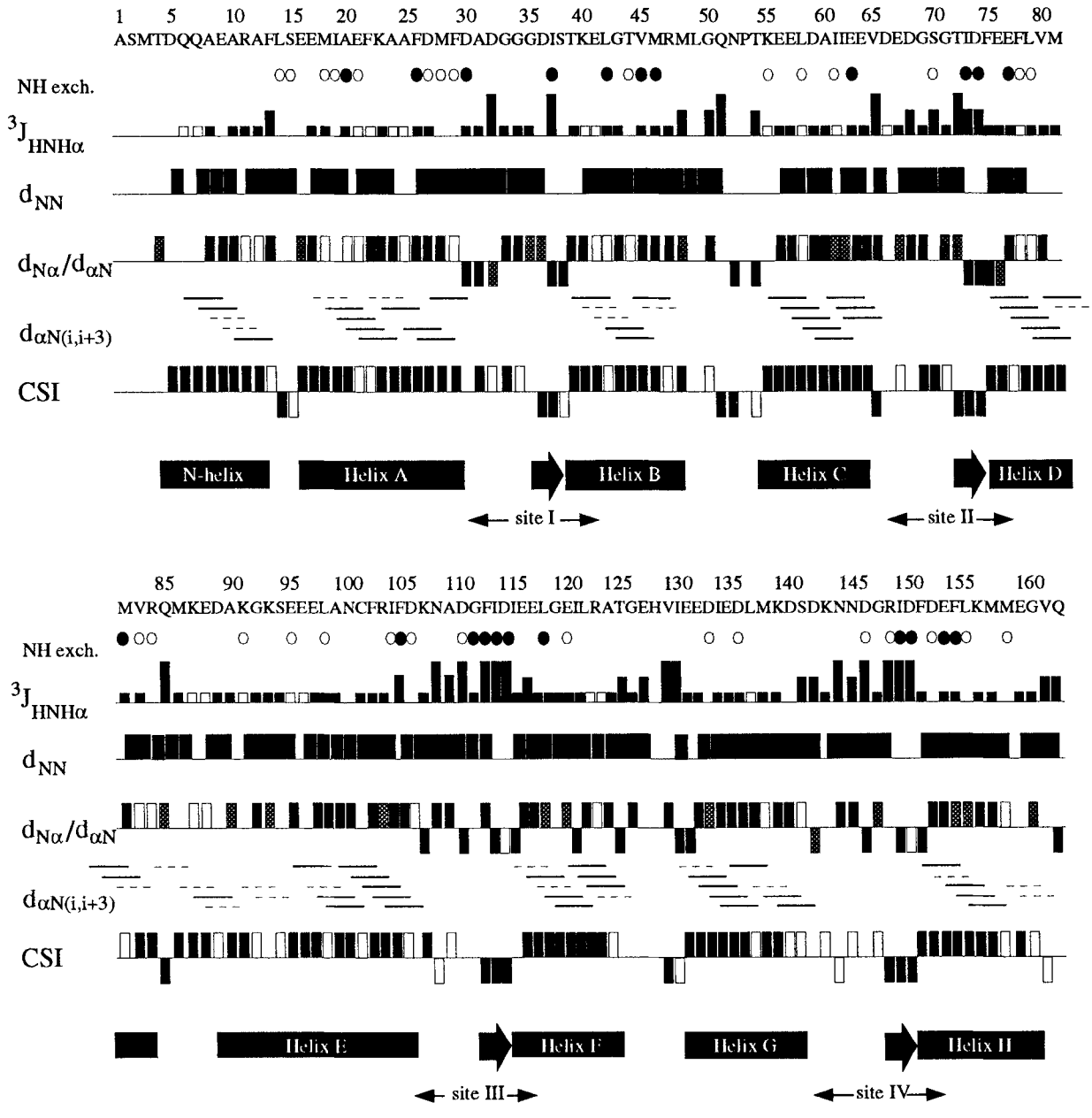

Fig. 3. Summary of TnC data on sequential and medium-range NOEs involving amide protons, ratio of the $d_{N\alpha}/d_{\alpha N}$ intensities, $^3J_{HNH\alpha}$ couplings, and CSI. The $d_{N\alpha}/d_{\alpha N}$ ratio represents the ratio between the $d_{N\alpha}(i, i)$ and the $d_{\alpha N}(i-1, i)$ NOE intensities. Boxes pointing up represent a ratio >1, and boxes pointing down represent a ratio <1. Unfilled boxes represent degeneracies in either the $d_{N\alpha}(i, i)$ or the $d_{\alpha N}(i-1, i)$ with other residues or with itself. Gray boxes represent ratios for which either the $d_{N\alpha}(i, i)$ or the $d_{\alpha N}(i-1, i)$ are missing, and it is assumed that the intensities are very small. No box means either that the ratio is approximately equal to 1, or that there was not enough information to determine the ratio (i.e., both the $d_{N\alpha}$ and $d_{\alpha N}$ are absent). The $^3J_{HNH\alpha}$ values are shown only if they are unambiguous (filled boxes) or ambiguous (unfilled boxes), when it is clear that no splitting can be observed. For the CSI, filled boxes pointing up indicate that all three chemical shift values ($^{13}C\alpha$, $^{13}C'$, and $^1H\alpha$) represent helix, filled boxes pointing down indicate that all three chemical shift values ($^{13}C\alpha$, $^{13}C'$, and $^1H\alpha$) represent β-sheet, and no box represents random coil chemical shifts. Unfilled boxes represent CSI values for which 2/3 represent that particular secondary structure. For the $d_{\alpha N}(i, i+3)$, the dotted lines represent an ambiguity. Secondary structure elements are marked according to the criteria shown, where boxes represent α-helix and arrows represent β-sheet. Unambiguous slowly exchanging amide resonances are shown with filled circles, whereas ambiguous slowly exchanging amide resonances are shown with unfilled circles. Residues and their numbering are indicated across the top.

close to the amide proton of the next residue (a distance of between 1.8 and 2.5 Å in β-sheets). α-Helices, however, have a much smaller intensity for the $d_{\alpha N}$ (the distance in α-helices between the NH(i) and CαH($i-1$) is between 3.3 and 3.6 Å). The $d_{N\alpha}/d_{\alpha N}$ ratio should thus provide us with a method for determining the secondary structure independent of the ^{15}N amide exchange rate or ^{15}N T_2 of that particular residue. The consensus of the CSI ($^{13}C\alpha$, $^{13}C'$, and $^1H\alpha$ chemical shift deviations

from random coil values) can predict to greater than 90% accuracy the secondary structure of a protein (Wishart & Sykes, 1994). The CSI, the $d_{N\alpha}/d_{\alpha N}$ ratio, the $d_{\alpha N}(i, i+3)$ NOEs and the J-coupling data therefore provide a very accurate determination of the secondary structure of TnC, which is summarized in Figure 3.

Comparison of the secondary structure of TnC with that of the crystal structure of TnC reveals striking similarities. The nine helices start and stop at approximately the same residue (Herzberg & James, 1988; Satyshur et al., 1988, 1994). The major difference in secondary structure occurs with the residue Glu 41, which is located in helix B. In the crystal structure, and in the secondary and tertiary structure of the apo N-domain (Gagné et al., 1994; S.M. Gagné, S. Tsuda, M.X. Li, L.B. Smillie, & B.D. Sykes, in prep.), helix B appears to have a break or kink at residue E41 (irregular ϕ/ψ angles). The B helix is thus started at residue 39, and continues to residue 40, breaks, then continues again at residue 42, as shown in Table 2. In the structure of calcium-saturated TnC and calcium-saturated NTnC (Gagné et al., 1994), E41 does not have irregular ϕ or ψ angles but is in a helical conformation (as supported by the d_{NN} NOEs, the $^3J_{HNH\alpha}$ coupling constants, as well as the CSI) (Table 2). The other differences are at the end of helix B, which occurs one residue sooner in the NMR-derived structure versus the crystal structure, and the four linker residues between the two domains found in the NMR structure. The observation of subtle changes in the N-domain on going from half to fully saturated TnC was first realized by Levine et al. (1977). They deduced from NMR studies at 270 MHz, that calcium binding to the low affinity sites causes changes in the environment of largely hydrophobic residues. The results were later verified by Levine et al. (1978), Evans et al. (1980), and Gagné et al. (1994).

The secondary structure of calmodulin has been determined (Ikura et al., 1991) using NMR and it was found to be very similar to that obtained for TnC. By aligning the calcium binding loops, very similar secondary structural elements and helix lengths were found. The numbering for calmodulin is different from the numbering for TnC by 10 residues in the N-domain (due to the lack of an N-terminal helix in calmodulin) and 13 residues in the C-domain (due to a difference of 3 residues in the linker between the two domains). In the calcium binding loops, there exists a short antiparallel β-sheet of three residues in both calmodulin and TnC. Table 2 illustrates the differences in the helices. For the most part, the helices in both calcium-saturated TnC and calmodulin are the same. The only difference occurs in the linker region, where calmodulin has six flexible residues versus three flexible residues for TnC (although Q85 has ϕ dihedral angles indicative of β-sheet structure, the ^{15}N T_2 data do not support flexibility for this residue). A comparison of residues in homologous positions in calmodulin and TnC reveals a 46% identity. Directly comparing the chemical shifts of these identical residues reveals that 81% of the backbone $^{13}C\alpha$ and $^{13}C'$ shifts are within 1 ppm and ^1H shifts are within 0.1 ppm. Including the backbone ^{15}N chemical shift (with an error of 1 ppm), the chemical shift similarity drops to 63%. For side-chain ^1H, ^{15}N, and ^{13}C chemical shifts, there is 75% identity between TnC and the identical residue in calmodulin (assuming a 1 ppm error for ^{13}C and ^{15}N chemical shifts and 0.1 ppm error for ^1H chemical shifts).

The secondary structure of the N-terminal domain of TnC is also very homologous to that obtained for the isolated N-domain (Gagné et al., 1994). The helix lengths are virtually identical, and the calcium binding loops are as well (Table 2). In terms of the similarity of assignment, 85% of the backbone chemical shifts and 87% of the side-chain chemical shifts of NTnC are identical with TnC (with the same errors as for the calmodulin comparison). The SCIII homodimer (Shaw et al., 1992) has 46% homology for the backbone chemical shifts and 50% for the side-chain chemical shifts, and the TH2 homodimer (Kay et al., 1989) has 44% for the backbone chemical shifts and 58% for the side-chain chemical shifts.

In this paper, we have described the details of the backbone ^1H, ^{13}C, and ^{15}N resonance assignments of TnC on the basis of the analysis of the 3D triple resonance experiments. These assignments were shown to be highly homologous to assignments made for calcium-saturated NTnC (Gagné et al., 1994), as well as to the structurally homologous protein calmodulin. Certainly this high homology suggests very similar secondary structure in terms of backbone chemical shifts but also suggests very similar tertiary structure as illustrated by the high homology in the side-chain chemical shifts. Secondary structure analysis of TnC confirms the supposition that the secondary structure of TnC is similar to these other structures. The elucidation of the 3D structure of TnC should confirm the similarity in tertiary structure of TnC to these other structures. Finally, it should be pointed out that the use of 15% (v/v) TFE to break up aggregation of TnC has not adversely affected the secondary or tertiary structure of TnC, thus reinforcing the use of TFE as a general perturbant of quaternary structure for stable proteins.

Table 2. *Comparison of α-helices*

	Residue range			
	TnC-4Ca^{2+}	TnC-2Ca^{2+}	CaM-4Ca^{2+}	NTnC-2Ca^{2+}
N-helix	5–13	3–13	n/a	5–13
Helix A	16–29	16–28	6–19	16–29
Helix B	39–48	39–40, 42–48	29–38	39–48
Helix C	55–64	55–64	45–54	55–64
Helix D	75–84	75–105	65–77	75–87
Helix E	89–105	75–105	82–93	n/a
Helix F	115–124	115–125	102–111	n/a
Helix G	131–141	131–141	118–127	n/a
Helix H	151–160	151–159	138–146	n/a

[a] TnC-4Ca^{2+} are helices found in the present study of calcium-saturated TnC. The helix range was based on the $^3J_{HNH\alpha}$, CSI, $d_{\alpha N}(i, i+3)$ NOE, and the $d_{N\alpha}/d_{\alpha N}$ NOE ratio. TnC-2Ca^{2+} are from Herzberg and James (1988). Helix limits were based on expected $^3J_{HNH\alpha}$ and NOEs from the crystal structure. CaM-4Ca^{2+} are helices as described in Ikura et al. (1991). NTnC-2Ca^{2+} are helices as described in Gagné et al. (1994).

Materials and methods

Sample preparation

TnC was cloned and expressed as described in Slupsky et al. (1995). Three TnC samples were prepared. The first sample was prepared by dissolving lyophilized ^{15}N,^{13}C-TnC in a buffer consisting of 150 mM KCl and 15 mM $CaCl_2$ in 99.5% D_2O at pH 7.6. This sample was lyophilized and redissolved in 99.5%

D_2O three times. After the last lyophilization step, the sample was dissolved in 85% D_2O and 15% TFE and the pH was adjusted with DCl to a pH of 7.0. This sample was used in the 3D HCACO, and the 2D NH exchange ^1H-^{15}N-HSQC experiments. The second sample was prepared by dissolving lyophilized ^{15}N,^{13}C-TnC in a buffer consisting of 150 mM KCl and 15 mM $CaCl_2$ in 75% H_2O, 10% D_2O, and 15% TFE (for use in the 3D HNCA, HNCO, HN(CO)CA experiments). The last sample was prepared by dissolving lyophilized ^{15}N-TnC in a buffer consisting of 150 mM KCl and 15 mM $CaCl_2$ in 75% H_2O, 10% D_2O, and 15% TFE (for use in the 3D ^{15}N-edited TOCSY, and ^{15}N-edited NOESY, and the 2D HMQC-J, and HSQC experiments). All samples had a pH of 7.0 and a protein concentration of approximately 1.4 mM, and a small amount of DSS was added to act as an internal standard. The pH of the D_2O sample was not corrected for isotope effects.

NMR spectroscopy

All NMR spectra were acquired at 40 °C on a Varian Unity 600 NMR spectrometer. The 2D ^1H-^{15}N HSQC spectrum (Bodenhausen & Reuben, 1980) was acquired using 64 complex points in t_1, and 1,024 complex points in t_2, with 64 scans per t_1 increment. The sweepwidths were 8,000 Hz (centered at the water frequency at 4.7 ppm) in F2 (^1H) and 1,824 Hz (centered at 119 ppm) in F1 (^{15}N). The spectrum was processed with a cosine-bell squared function in F2 and a Lorentzian-Gaussian function in F1, and both dimensions were zero-filled to 2,048 points. The 2D HMQC-J (Kay & Bax, 1990) spectrum was acquired with 848 complex points in t_1 and 1,024 complex points in t_2, with 128 scans per t_1 increment. The sweepwidths were 8,000 Hz (centered at the water frequency at 4.7 ppm) in F2 (^1H) and 1,824 Hz (centered at 119 ppm) in F1 (^{15}N). The spectrum was processed with a cosine-bell squared function and zero-filling to 2,048 points in F2 and a series of line broadenings together with a Gaussian function and zero-filling to 4,096 points in F1. The VNMR (VNMR 4.1A; Varian, Palo Alto, California) parameters used in F1 were either GF = 0.105, and LB = −10, −9, −8, −7, −6, −5, −4, −3, −2, and −1, or GF = 0.068, and LB = −18, −17, −16, −15, −14, −13, −12, −11, −10, −9, −8, −7, −6, −5, and −4. The splittings (in Hz) at the various LB values were fit with the program HMCQJFIT (Goodgame & Geer, 1993), which was modified for use with VNMR parameters to obtain the $^3J_{HNH\alpha}$ coupling constants. Coupling constants derived from both sets of weighting functions were within 0.5 Hz of one another, indicating that the coupling constants derived were accurate to approximately 0.5 Hz. For the NH exchange experiments, the $^{13}C/^{15}N$ TnC sample, which had been lyophilized three times in D_2O at a pH of 7.6, was used. Three spectra were acquired: one 3 h after final dissolution in 85% D_2O and 15% TFE and pH 7.0, one 3 days after dissolution, and one 3 weeks after dissolution. The spectra collected were ^1H-^{15}N-HSQC experiments with sweepwidths and carrier positions as indicated above for the ^1H-^{15}N-HSQC spectrum. The spectra were 512 (F2) × 128 (F1) complex points with 96 transients per increment. Presaturation of the small residual HOD peak was removed by application of a low power (γB_2 = 0.02 kHz) presaturation pulse of 1.4 s duration. The spectra were processed with a cosine-bell squared function in F2 and a Lorentzian-Gaussian resolution enhancement function in F1 with zero-filling to 2,048 points in both dimensions.

For backbone assignment of TnC, the following spectra were acquired: 3D HNCA (Grzesiek & Bax, 1992), 3D HN(CO)CA (Grzesiek & Bax, 1992), 3D HNCO (Grzesiek & Bax, 1992), 3D HCACO (Powers et al., 1991), 3D ^{15}N-edited TOCSY (75 ms mixing time) (Marion et al., 1989b), and 3D ^{15}N-edited NOESY experiments (75 ms mixing time) (Kay et al., 1989). All spectra were acquired with the proton carrier centered on the water frequency (4.70 ppm), and water suppression was by either a low power (γB_2 = 0.02 kHz) presaturation pulse of approximately 1.5 s duration or by spin lock (HN(CO)CA spectrum only) water suppression (Messerle et al., 1989), or for the HCACO experiment, no form of water suppression was needed. Sweepwidths for the proton dimension were 8,000 Hz, except for the HCACO experiment (3,000 Hz). For those spectra edited by ^{15}N in F2, the sweepwidth used was 1,824 Hz (or 2,100 Hz for the HN(CO)CA experiment) centered at 119 ppm. The sweepwidths of the ^{13}C dimension were as follows: for the HNCA, the sweepwidth was 3,922 Hz with the carrier centered at 56 ppm; for the HN(CO)CA, the sweepwidth was 4,500 with the carrier centered at 177.8 ppm; for the HNCO experiment, the sweepwidth was 1,818 Hz, with the carrier centered at 177.8 ppm; and for the HCACO experiment, the sweepwidth was 4,564 Hz (F1) and 1,818 Hz (F2) with the carrier centered at 56 ppm. The HNCA experiment was collected with 32 (t_1) × 32 (t_2) × 512 (t_3) complex points with 192 scans per increment, the HN(CO)CA and HNCO experiments were collected with 28 (t_1) × 32 (t_2) × 512 (t_3) complex points with 192 scans per increment, the HCACO experiment was collected with 28 (t_1) × 48 (t_2) × 512 (t_3) complex points and 128 scans per increment, and the ^{15}N-edited NOESY and the ^{15}N-edited TOCSY experiments were acquired with 128 (t_1) × 32 (t_2) × 512 (t_3) complex points and either 64 scans per increment or 32 scans per increment (^{15}N-edited TOCSY).

For the HNCA, HN(CO)CA, HNCO, and HCACO experiments, the time domain was increased by 32 complex points in both the F2 and F1 dimensions by means of linear prediction and zero-filling, so that after processing, the spectrum had a size of 1,024(F3)*128(F1)*64(F2) points. The ^{15}N-edited TOCSY and the ^{15}N-edited NOESY experiments were linear predicted in F2 only, and after processing, the final size of the spectra was 1,024(F3)*256 (F1)*64(F2) points. For all experiments (except the HCACO), a postacquisition solvent suppression by convolution of the time-domain data was applied prior to Fourier transformation (Marion et al., 1989a). All spectra were processed with either a cosine-bell squared or a 60°-shifted sine-bell squared weighting function in F1 and F2, and a cosine-bell squared weighting function in F3. After Fourier transformation of the F3 dimension, parts of the spectra without resonances were discarded, reducing the final size to between 50% and 75%.

Processing of the 3D data sets was accomplished using either the VNMR software (VNMR 4.1A; Varian, Palo Alto, California) or NMRPIPE (F. Delaglio, NIDDK, NIH, Bethesda, Maryland, unpubl.). When used within VNMR software, extension of the time domain was achieved using the linear prediction algorithm lpfft. Peak picking was carried out using the interactive graphic-based program PIPP (Garrett et al., 1991).

Assignment of backbone ^1H, ^{15}N, and ^{13}C NMR chemical shifts

The sequential assignment of TnC was started with the HNCA experiment where the more intense $^1HN(i)$-$^{15}N(i)$-$^{13}C\alpha(i)$

correlation was observed. Sequential assignment was continued to the previous residue using a combination of the weaker correlation (due to the smaller two-bond coupling to the previous residue) found on the HNCA experiment coupled with the HN(CO)CA experiment at the same ^{15}N and ^{1}HN frequencies. Both the HNCA and the HN(CO)CA experiments provide the $^{1}HN(i)$-$^{15}N(i)$-$^{13}C\alpha(i-1)$ correlation. The $d_{NN}(i \pm 1)$ information obtained from the ^{15}N-edited NOESY experiment, together with the $^{1}HN(i)$-$^{15}N(i)$-$^{13}C'(i-1)$ correlation from the HNCO experiment are also needed. The $^{13}C'(i-1)$ information, coupled with the $^{13}C\alpha(i-1)$ information, can be used in the HCACO experiment to obtain the $^{1}H\alpha(i-1)$ correlation. The $^{1}H\alpha(i-1)$, the $^{1}HN(i \pm 1)$, and the $^{13}C\alpha(i-1)$ information obtained can then be used to search for all possible ^{15}N-^{1}H amide pairs in the ^{15}N-edited TOCSY, ^{15}N-edited NOESY, and HNCA experiments that best correlate residue i to residue $i-1$. Because of overlap in both the ^{1}H-^{15}N dimensions and the $^{1}H\alpha$-$^{13}C\alpha$ dimensions, the procedure frequently yielded multiple possibilities. When this was the case, the sequential assignment was continued from another place.

Acknowledgments

We thank Dr. Dan Garrett, Dr. Frank Delaglio, and the Laboratory of Chemical Physics at the National Institutes of Health for making available the programs PIPP and NMRPIPE, which were useful for analyzing and processing our NMR data. We are grateful to Mr. Stéphane Gagné for many insightful discussions and for a critical reading of the manuscript.

References

Babu A, Rao VG, Su H, Gulati J. 1993. Critical minimum length of the central helix in troponin C for the Ca^{2+} switch in muscular contraction. *J Biol Chem 268*:19232–19238.

Barbato G, Ikura M, Kay LE, Pastor RW, Bax A. 1992. Backbone dynamics of calmodulin studied by ^{15}N relaxation using inverse detected two-dimensional NMR spectroscopy: The central helix is flexible. *Biochemistry 31*:5269–5278.

Bax A, Clore GM, Driscoll PC, Gronenborn AM, Ikura M, Kay LE. 1990a. Practical aspects of proton-carbon-carbon-proton three-dimensional correlation spectroscopy of ^{13}C labeled proteins. *J Magn Reson 87*:620–627.

Bax A, Clore GM, Gronenborn AM. 1990b. Removal of F_1 baseline distortion and optimization of folding in multidimensional NMR spectra. *J Magn Reson 91*:174–178.

Bodenhausen G, Reuben DJ. 1980. Natural abundance nitrogen-15 NMR by enhanced heteronuclear spectroscopy. *Chem Phys Lett 69*:185–188.

Clore GM, Gronenborn AM. 1991. Structures of larger proteins in solution: Three- and four-dimensional heteronuclear NMR spectroscopy. *Science 252*:1390–1399.

Dobrowolski Z, Xu G, Chen W, Hitchcock-DeGregori SE. 1991. Analysis of the regulatory and structural defects of troponin C central helix mutants. *Biochemistry 30*:7089–7096.

Evans JS, Levine BA, Leavis PC, Gergely J, Grabarek Z, Drabikowski W. 1980. Proton magnetic resonance studies on proteolytic fragments of troponin C. Structural homology with the native molecule. *Biochim Biophys Acta 623*:10–20.

Fujimori K, Sorenson M, Herzberg O, Moult J, Reinach FC. 1990. Probing the calcium-induced conformational transition of troponin C with site-directed mutants. *Nature 345*:182–184.

Gagné SM, Tsuda S, Li MX, Chandra M, Smillie LB, Sykes BD. 1994. Quantification of the calcium-induced secondary structural changes in the regulatory domain of troponin C. *Protein Sci 3*:1961–1974.

Garrett DS, Powers R, Gronenborn AM, Clore GM. 1991. A common sense approach to peak picking in two-, three-, and four-dimensional spectra using automatic computer analysis of contour diagrams. *J Magn Reson 95*:214–220.

Goodgame MM, Geer SM. 1993. HMQCJFIT-software for analyzing HMQC-J spectra. *J Magn Reson Ser A 102*:246–248.

Grabarek Z, Tan R, Wang J, Tao T, Gergely J. 1990. Inhibition of mutant troponin C activity by an intra-domain disulphide bond. *Nature 345*:132–135.

Grabarek Z, Tao T, Gergely J. 1992. Molecular mechanism of troponin-C function. *J Muscle Res Cell Motil 13*:383–393.

Gronenborn AM, Clore GM. 1994. Where is NMR taking us? *Proteins Struct Funct Genet 19*:273–276.

Grzesiek S, Bax A. 1992. Improved 3D triple-resonance NMR techniques applied to a 31 kDa protein. *J Magn Reson 96*:432–440.

Gulati J, Babu A, Su H, Zhang Y. 1993. Identification of regions conferring calmodulin-like properties to troponin C. *J Biol Chem 268*:11685–11690.

Gulati J, Persechini A, Babu A. 1990. Central helix role in the contraction-relaxation switching mechanisms of permeabilized skeletal and smooth muscles with genetic manipulation of calmodulin. *FEBS Lett 263*:340–344.

Gusev NB, Grabarek Z, Gergely J. 1991. Stabilization by a disulfide bond of the N-terminal domain of a mutant troponin C (TnC48/82). *J Biol Chem 266*:16622–16626.

Heidorn DB, Trewhella J. 1988. Comparison of the crystal and solution structures of calmodulin and troponin C. *Biochemistry 27*:909–915.

Herzberg O, James MNG. 1988. Refined crystal structure of troponin C from turkey skeletal muscle at 2.0 Å resolution. *J Mol Biol 203*:761–779.

Herzberg O, Moult J, James MNG. 1986. A model for the Ca^{2+} induced conformational transition of troponin C. *J Biol Chem 261*:2638–2644.

Ikura M, Kay LE, Bax A. 1990a. A novel approach for sequential assignment of ^{1}H, ^{13}C, and ^{15}N spectra of larger proteins: Heteronuclear triple-resonance three-dimensional NMR spectroscopy: Application to calmodulin. *Biochemistry 29*:4659–4667.

Ikura M, Kay LE, Tschudin R, Bax A. 1990b. Three-dimensional NOESY-HMQC spectroscopy of a ^{13}C-labeled protein. *J Magn Reson 86*:204–209.

Ikura M, Spera S, Barbato G, Kay LE, Drinks M, Bax A. 1991. Secondary structure and side-chain ^{1}H and ^{13}C resonance assignments of calmodulin in solution by heteronuclear multidimensional NMR spectroscopy. *Biochemistry 30*:9216–9228.

Kay LE, Bax A. 1990. New methods for the measurement of NH-CαH coupling constants in ^{15}N-labeled proteins. *J Magn Reson 86*:110–126.

Kay LE, Forman-Kay JD, McCubbin WD, Kay CM. 1991. Solution structure of a polypeptide dimer comprising the fourth Ca^{2+}-binding site of troponin C by nuclear magnetic resonance spectroscopy. *Biochemistry 30*:4323–4333.

Kay LE, Marion D, Bax A. 1989. Practical aspects of 3D heteronuclear NMR of proteins. *J Magn Reson 84*:72–84.

Levine BA, Mercola D, Coffman D, Thornton JM. 1977. Calcium binding by troponin C. A proton magnetic resonance study. *J Mol Biol 115*:743–760.

Levine BA, Thornton JM, Fernandes R, Kelly CM, Mercola D. 1978. Comparison of the calcium and magnesium induced structural changes of troponin C. A proton magnetic resonance study. *Biochim Biophys Acta 535*:11–24.

Li MX, Gagné SM, Tsuda S, Kay CM, Smillie LB, Sykes BD. 1995. Calcium binding to the regulatory N domain of skeletal muscle troponin C occurs in a step-wise manner. *Biochemistry*. Forthcoming.

Marion D, Driscoll PC, Kay LE, Wingfield PT, Bax A, Gronenborn AM, Clore GM. 1989a. Overcoming the overlap problem in the assignment of ^{1}H NMR spectra of larger proteins by use of three-dimensional heteronuclear ^{1}H-^{15}N Hartmann–Hahn-multiple quantum coherence and nuclear Overhauser multiple quantum coherence spectroscopy: Application to interleukin 1β. *Biochemistry 28*:6150–6156.

Marion D, Kay LE, Sparks SE, Torchia DA, Bax A. 1989b. Three-dimensional heteronuclear NMR of ^{15}N labeled proteins. *J Am Chem Soc 111*:1515–1517.

Meadows RP, Olejniczak ET, Fesik SW. 1994. A computer-based protocol for semiautomated assignments and 3D structure determination of proteins. *J Biol NMR 4*:79–86.

Means AR, Dedman JR. 1980. Calmodulin–An intracellular calcium receptor. *Nature 285*:73–77.

Messerle B, Wider G, Otting G, Weber C, Wüthrich K. 1989. Solvent suppression using a spin lock in 2D and 3D NMR spectroscopy with H_2O solutions. *J Magn Reson 85*:608–613.

Olah GA, Trewhella J. 1994. A model structure of the muscle protein complex $4Ca^{2+}$·troponin C·troponin I derived from small-angle scattering data: Implications for regulation. *Biochemistry 33*:12800–12806.

Pearlstone JR, Borgford T, Chandra M, Oikawa K, Kay CM, Herzberg O, Moult J, Herklotz A, Reinach RC, Smillie LB. 1992a. Construction and characterization of a spectral probe mutant of troponin C: Application to analyses of mutants with increased Ca^{2+} affinity. *Biochemistry 31*:6545–6553.

Pearlstone JR, McCubbin WD, Kay CM, Sykes BD, Smillie LB. 1992b. Spectroscopic analysis of a methionine-48 to tyrosine mutant of chicken troponin C. *Biochemistry 31*:9703–9708.

Potter JD, Gergely J. 1975. The calcium and magnesium binding sites on troponin and their role in the regulation of myofibrillar adenosine triphosphate. *J Biol Chem 263*:2371–2376.

Powers R, Gronenborn AM, Clore GM, Bax A. 1991. Three-dimensional triple-resonance NMR of $^{13}C/^{15}N$-enriched proteins using constant-time evolution. *J Magn Reson 94*:209–213.

Reinach FC, Karlsson R. 1988. Cloning, expression, and site-directed mutagenesis of chicken skeletal muscle troponin C. *J Biol Chem 263*:2371–2376.

Satyshur KA, Pyzalska D, Greaser M, Rao ST, Sundaralingam M. 1994. Structure of chicken skeletal muscle troponin C at 1.78 Å resolution. *Acta Crystallogr D 50*:40–49.

Satyshur KA, Rao ST, Pyzalska D, Drendel W, Greaser M, Sundaralingam M. 1988. Refined structure of chicken skeletal muscle troponin C in its two calcium state at 2.0 Å resolution. *J Biol Chem 263*:1628–1647.

Shaw GS, Hodges RS, Sykes BD. 1990. Calcium-induced peptide association to form an intact protein domain: ^{1}H-NMR structural evidence. *Science 249*:280–283.

Shaw GS, Hodges RS, Sykes BD. 1992. Determination of the solution structure of a synthetic two-site calcium-binding homodimeric protein domain by NMR spectroscopy. *Biochemistry 31*:9572–9580.

Slupsky CM, Kay CM, Reinach FC, Smillie LB, Sykes BD. 1995. The calcium-induced dimerization of troponin C: The mode of interaction and the use of trifluoroethanol as a denaturant of quaternary structure. *Biochemistry 34*. Forthcoming.

Tsuda S, Hasegawa Y, Yoshida M, Yagi K, Hikichi K. 1988. Nuclear magnetic resonance study on rabbit skeletal troponin C: Calcium induced conformational change. *Biochemistry 27*:4120–4126.

Tsuda S, Ogura K, Hasegawa Y, Yagi K, Hikichi K. 1990. ^{1}H NMR study of rabbit skeletal muscle troponin C: Mg^{2+}-induced conformational change. *Biochemistry 29*:4951–4958.

Wagner G. 1993. Prospects for NMR of large proteins. *J Biomol NMR 3*:375–385.

Wang C, Liao R, Cheung HC. 1993. Rotational dynamics of skeletal muscle troponin C. *J Biol Chem 268*:14671–14677.

Wishart DS, Sykes BD. 1994. The ^{13}C chemical shift index: A simple method for the identification of protein secondary structure using ^{13}C chemical shift data. *J Biomol NMR 4*:171–180.

Wishart DS, Sykes BD, Richards FM. 1991a. Simple techniques for the quantification of protein secondary structure by ^{1}H NMR spectroscopy. *FEBS Lett 293*:72–80.

Wishart DS, Sykes BD, Richards FM. 1991b. Relationship between nuclear magnetic resonance chemical shift and protein secondary structure. *J Mol Biol 222*:311–333.

Wüthrich K. 1986. *NMR of proteins and nucleic acids*. New York: John Wiley & Sons.

Xu G, Hitchcock-DeGregori SE. 1988. Synthesis of a troponin C cDNA and expression of wild-type and mutant proteins in *Escherichia coli*. *J Biol Chem 263*:13962–13969.